B. Ramakrishnan

L. Zhu

R. Pitchumani[1]
Mem. ASME
e-mail: pitchu@engr.uconn.edu

Composites Processing Laboratory,
Department of Mechanical Engineering,
University of Connecticut, U-139,
Storrs, CT 06269-3139

Curing of Composites Using Internal Resistive Heating

Curing of fiber-resin mixtures is often the critical and productivity controlling step in the fabrication of thermosetting-matrix composites. The long processing times (and costs) have remained the fundamental impediment to widespread commercialization of composites. Shortening the cure cycle time, while ensuring a complete and uniform cure in the product, is imperative for realizing the goal of affordable materials processing, and forms the focus of this investigation. Toward addressing the affordability challenge, this paper explores the use of conductive carbon mats embedded inside the composite as a means of providing internal volumetric resistance heating during the cure process. The supplemental heating results in temperature and cure uniformity through the cross section, as well as speeds up the cure process. In the context of application to resin transfer molding, systematic experimental and theoretical studies on various resistive heating configurations are presented. Optimum processing strategies are derived based on the cure time and microstructural product quality considerations. [S1087-1357(00)01101-1]

Introduction

Fabrication of reinforced thermosetting composites is accomplished using techniques such as pultrusion, autoclave curing, and resin transfer molding, all of which share the common and critical step of cure. During the cure process the resin-saturated preform is exposed to a prescribed temperature schedule—referred to as a cure cycle—which initiates and sustains a cross-linking polymerization reaction of the resin and transforms the fiber-resin mixture into a structurally hard composite product. In typical processing, the cure times could be on the order of hours, depending upon the part thickness. An important objective of commercial composites fabrication is that of reducing the manufacturing time (and cost). Significant reduction in the overall processing times can be realized through a shortened cure cycle time, while ensuring a complete and uniform cure of the product.

During the cure process, the outer layers of the laminate, which are subject to external heating, cure far more rapidly than the inner layers, which are heated primarily by conduction from the outer layers. The differential curing rates are especially significant in thick sections, where the differential leads to structurally poor products. Toward addressing the above problem, alternative curing strategies using microwave energy have been explored [1–3]. However, since microwave energy attenuates with thickness, the problem of differential curing persists, although alleviated slightly in comparison to conventional curing. As a result, the approach adopted in practice is the use of cure cycles with lower temperatures and longer cycle durations, thereby leaving the objective of rapid and affordable composite processing yet to be realized.

The shortcomings of existing cure strategies in regard to differential curing and long cure cycle times may be avoided if the composite laminate being cured were to be heated from *within* the cross section, in conjunction with peripheral heating. One approach to realizing this is the use of conductive fibers, such as carbon, as heating elements embedded within the laminate. The passage of electric current through the conductive fibers causes resistive internal heating which provides for a uniform curing through the thickness. Physically, this approach reduces to effectively dividing the thick composite section into a number of thinner sections, each of which is cured uniformly by resistance heating from the conducting fibers. Moreover, since the total energy used in curing the composite is increased, the cure cycle times can be reduced. The conductive fibers are left embedded in the composite, since they are structural reinforcements as well.

Initial studies on demonstrating the concept feasibility have been reported previously [4,5]. For a viable practical implementation, however, a detailed understanding of the process is required. Toward this end, it is the intent of this study to (a) conduct a systematic experimental investigation of the effects of the number of resistive heating elements, their placement, and the power supplied to them on the fabrication time and parameters influencing the product quality, (b) develop a theoretical model describing the process, and to validate it with the experimental data, and (c) derive processing windows and optimum supplemental configurations from the investigations.

The experimental investigation is presented in the context of the resin transfer molding process, although the underlying methodology and results are generically applicable to other cure processes as well. A numerical model accounting for internal heat generation due to the chemical reaction and the resistive heating from the embedded carbon mats is developed to simulate the process. The productivity enhancements afforded by the resistive heating approach are elucidated through comparison with the case of conventional curing. Furthermore, microstructural evaluation was conducted on the fabricated specimens in order to assess the influence of the supplemental heating on the product quality. A processing window, identified based on quality constraints, is presented which provides the feasible range of power input as a function of the number of carbon mat layers.

The organization of the paper is as follows: A description of the resistive heating experimental setup is presented first, followed by the studies on resin kinetics characterization, the thermochemical model used for a theoretical simulation of the configurations studied experimentally, and the results of the study.

Experimental Studies

Experimental studies were conducted to (a) investigate the effects of three parameters—the number and the location of the resistive carbon mats embedded inside the composite, and the power supplied—on the cure time and the parameters influencing the composite quality, and (b) obtain a processing window, and identify the optimal processing conditions. A lab-scale resin transfer molding (RTM) setup, shown schematically in Fig. 1, was used for conducting the experiments. The resin transfer molding process has three stages, beginning with the stacking up of several layers of tailored fiber mats into an enclosed mold. The second

[1]Author to whom correspondence must be addressed.

Contributed by the Manufacturing Engineering Division for publication in the JOURNAL OF MANUFACTURING SCIENCE AND ENGINEERING. Manuscript received December 1998; revised June 1999. Associate Technical Editor: R. Smelser.

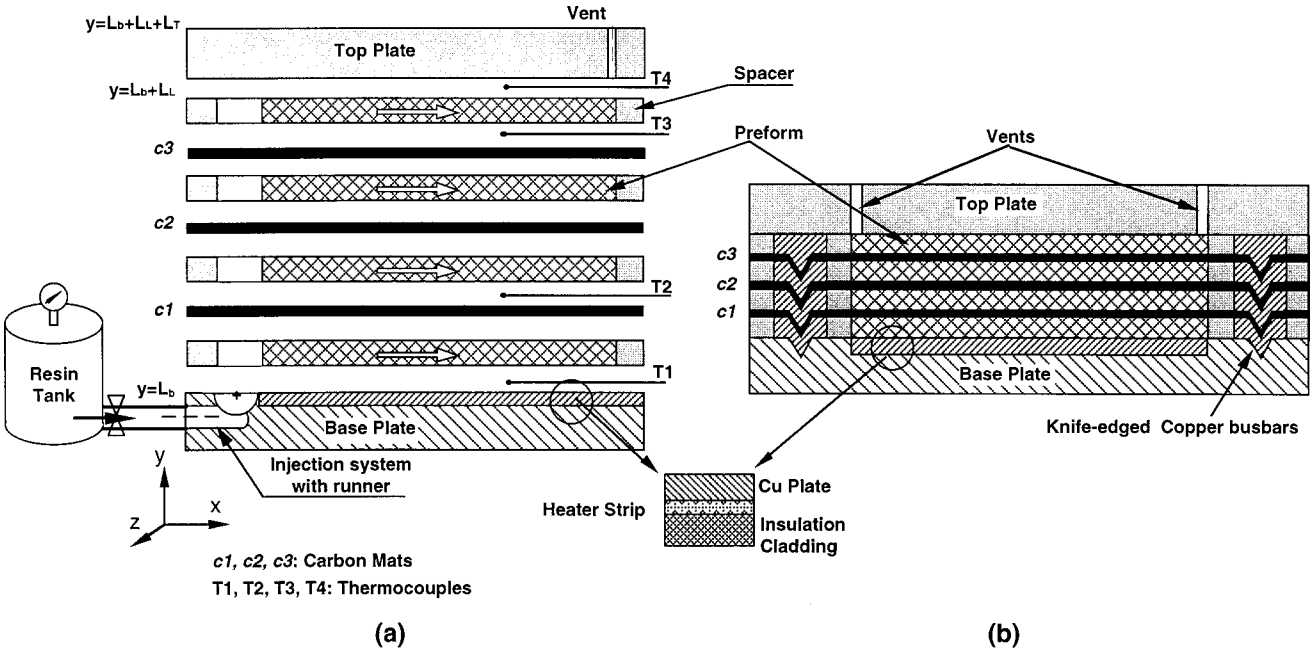

Fig. 1 Schematic of the experimental setup used for the resistive heating studies

step includes the injection of a catalyzed resin mixture, and its uniform permeation into the porous medium formed by the stacked fiber bed (known as a preform). Finally, the whole system is heated, expediting the curing of the resin.

The main components of the experimental setup include a pressure tank that houses the catalyzed resin and a mold in which the preform is placed. The mold consists of a sandwich construction of a bottom base plate, a stack of picture-frame spacers which determine the laminate thickness, and a top plate, all made using Teflon. Teflon was selected based on its (a) ease of machinability, (b) very low thermal and electrical conductivity, and (c) inertness toward the epoxy resin system, which facilitates demolding. The base plate is comprised of a resin inlet port which is a 0.25 in. diameter tapped hole that discharges into a concave runner along the width of the mold, as illustrated in Fig. 1(*a*). The runner ensures a uniform, essentially one-dimensional permeation of the preform along the mold length. As shown in Fig. 1(*a*), the Teflon mold additionally incorporates a cavity, which houses a strip heater, for surface heating of the resin-saturated preform. The heater cavity is closed by a copper plate that houses the thermocouples and ensures uniform surface heating of the composite. The copper plate was surface ground to a smooth finish in order to minimize the surface interaction with the resin flow during the process, and was mounted flush with the surface of the Teflon base plate.

The experiments were conducted for a mold cavity (composite) thickness of 0.5 in., which was formed using four spacers of 0.125 in. thickness each. Note that since the top Teflon plate acts as an insulating surface, the arrangement studied also simulates the case of symmetric curing of a 1 in. thick composite. The use of four spacers provided for the incorporation of up to three resistive heating patches through the thickness of the preform. Slots were cut along the sides of the spacer frames in order to accommodate knife-edged, stackable copper bus bars along the length of the mold (i.e., the *x* direction in Fig. 1). Each bus bar had a V-shaped knife edge and a matching V-shaped groove machined along its length, as shown in the cross-sectional view of the mold in Fig. 1(*b*), such that the bus bars could be stacked pefectly on top of one another. The carbon mats were secured tightly in place between the knife edge and the mating groove of adjacent bus bars, as illustrated in Fig. 1(*b*). This arrangement ensured firm contact between the bus bars and the carbon mats throughout their length, and provided for uniform distribution of the power supplied from the source. The heating uniformity of the carbon mats was verified in separate experiments using an infrared thermal imaging camera focused on the plane of the carbon mats.

The power source supplied dc power with an adjustable voltage of 0 to 20 V. Since the carbon mats were connected in a parallel arrangement to the power source, the total current was distributed equally among them. The low permeability of the carbon mats combined with the tight clamping and sealing of the spacer assembly served to eliminate any leakage of the resin from the sides of the mold during the infiltration process. In order to measure temperature variation through the thickness, each of the spacers also had slots cut through them on the side opposite the injection port to house the thermocouple wires. The top plate, made of 0.5 in. thick Teflon, included two air vents drilled to be in-line with the corners of the mold cavity furthest from the injection face, as shown in Fig. 1(*a*). The overall sandwich setup was secured by four snap clamps.

Control of the surface heater mounted on the base plate of the mold was accomplished with a solid state relay which was regulated by a proportional integral derivative (PID) control scheme implemented in LabVIEW [6]. Temperature signals measured on the base plate and through the thickness of the mold by the thermocouples were acquired via a terminal block to an NB-MIO-16L-9 National Instruments data acquisition (DAQ) board. The heating control was achieved by suitably adjusting the ''on'' (closed) and the ''off'' (open) duration of the solid state relay. Accordingly the 0 percent–100 percent output signal from the PID controller was scaled to control the length of time that the system heater remained at full power. The temperature through the thickness of the mold was recorded at the positions $T1$, $T2$, $T3$, and $T4$, as shown in Fig. 1(*a*), every 2 s. The temperature readings were used to compute the degree of cure in the composite, through its thickness, using the empirical kinetics model for the resin system, which was developed as explained in the next section. The time required for the composite to reach a cure of 97 percent throughout the cross section was considered to be the cure time.

Continuous glass strand mat, M8610, supplied by the Owens-Corning Fiberglass Corporation was used as the reinforcement

material in all the experiments. Carbon mats, G-104, supplied by Textile Technologies, Inc., were used as the resistive heating elements. The heating studies were conducted using epoxy resin, EPON-815, catalyzed with Epicure 3274, both supplied by the Shell Chemical Company. The resin selection for the study was based on its low viscosity, which permitted quick mold fills using relatively low injection pressures. The resin cure characteristics were obtained using differential scanning calorimetry explained in detail in the following section.

Resin Cure Kinetics

Information on resin kinetics is required for (a) monitoring the degree of cure during the process as explained in the previous section, and (b) describing the exothermic source term in the thermal model presented in the next section. Since the kinetic parameters of the resin-catalyst mixture, EPON 815/Epicure 3274, were not available in the open literature, nor from the manufacturer, they were characterized using differential scanning calorimetry (DSC). The goal of the characterization studies was to obtain an empirical expression for the cure rate of the form

$$d\alpha/dt=(K_1+K_2\alpha^m)(1-\alpha)^n \tag{1}$$

which is shown in the literature to describe well the experimentally observed rate of cure for epoxy resins [7–9]. In the above equation, α denotes a degree of cure defined as the fraction of the initial resin concentration that has reacted at a time instant, t, m, and n are empirical exponents, and K_1 and K_2 are the rate constants that vary with the temperature, T, following the Arrhenius relationship

$$K_1=k_{10}e^{-E_1/RT};\quad K_2=k_{20}e^{-E_2/RT} \tag{2}$$

in which k_{10} and k_{20} are frequency factors, E_1 and E_2 are activation energies, and R is the universal gas constant.

The approach to obtaining the kinetic parameters followed a standard procedure as given by Han et al. [7]. The principal steps in the procedure are outlined below and the reader is referred to Han et al. [7] for further details. First, the heat generated during the cure reaction was measured by completing the reaction nonisothermally in which a predetermined amount of resin was heated in a differential scanning calorimeter from room temperature at the rate of 10°C/min until there was no more heat being generated by reaction (at about 200°C). Figure 2 shows the rate of heat generated, dQ/dt, as a function of time, t, referred to as a thermogram, for the nonisothermal DSC run. The total heat generated due to the reaction, H_R, was obtained as the area under the thermogram by integrating the measured heat flow with respect to time. The heat of the reaction, H_R, for the EPON 815/Epicure 3274 system was determined to be 384 J/g.

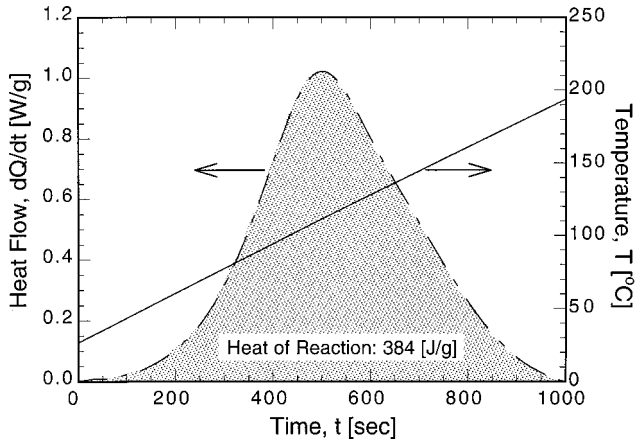

Fig. 2 Determination of the heat of reaction, based on a nonisothermal DSC scan

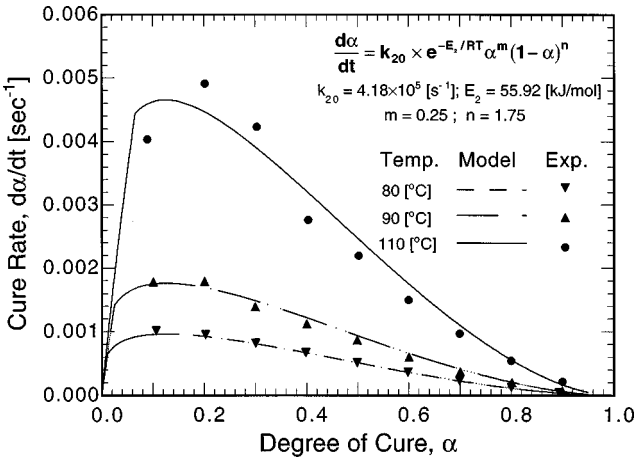

Fig. 3 Model parameters for the kinetics of the EPON 815/ EPICURE 3274 resin/catalyst system, obtained from isothermal DSC scans.

Isothermal scans on the resin system were conducted to obtain dQ/dt versus time, t, for various temperatures in the range 80°C to 110°C. The value for H_R obtained above was also confirmed from the area under the isothermal thermograms. Since the total amount of heat generated by the cure reaction at any time, $Q(t)$, is directly proportional to the degree of cure, α, of the sample at that particular instant, the rate of cure, $d\alpha/dt$, can be defined as

$$\frac{d\alpha}{dt}=\frac{1}{H_R}\frac{dQ(t)}{dt} \tag{3}$$

Using the above relationship, the isothermal thermograms were cast as plots of $d\alpha/dt$ versus time, t, and the degree of cure, α, was obtained by integrating these plots with respect to time. Figure 3 shows the cure rate, $d\alpha/dt$, as a function of the degree of cure, α, at a selected few of the various isothermal conditions studied. The empirical parameters in the kinetics equation (Eqs. (1) and (2)) were then obtained as follows: first, the $d\alpha/dt$ versus α data for each temperature was fitted to the right-hand side of Eq. (1) to determine K_1, K_2, m, and n. The natural logarithms of K_1 and K_2 were then plotted against $1/T$ [K^{-1}] to obtain k_{10}, k_{20}, E_1, and E_2. For the EPON 815/Epicure 3274 resin system, the value of K_1 was determined to be zero, while the values of k_{20}, E_2, m, and n are summarized in Fig. 3.

Process Model

A numerical thermochemical model was developed to describe the cure process with supplemental internal resistive heating. The process phenomena involved are (1) the heat transfer associated with the heating of the fiber-resin mixture, including the effects of the heat of the exothermic cure reaction and the resistive heating of the carbon mats, coupled with (2) the kinetics of the cure reaction, described by the Arrhenius-type empirical relationship in Eq. (1).

The thermal model consists of solving the energy equation in Cartesian coordinates for the temperature distribution through the mold cross section. Assuming the heating to be uniform across the width and the length of the mold (x and z directions in Fig. 1), the energy transfer is predominantly one-directional through the mold thickness (y direction in Fig. 1). The governing equation, therefore, for the one-dimensional heat transfer in the three-material domain (formed by the copper base plate, the resin-saturated preform layers, and the top Teflon cover), accounting for the internal heat generation due to the exothermic cure reaction and due to the resistive heating of the embedded carbon mat in the composite, may be written as

$$\frac{\partial[(\rho CT)_b]}{\partial t}=\frac{\partial}{\partial y}\left(k_b\frac{\partial T_b}{\partial y}\right};\quad 0\leqslant y\leqslant L_b\ \text{(copper base plate)}$$

$$\frac{\partial[(\rho CT)_L]}{\partial t}=\frac{\partial}{\partial y}\left(k_L\frac{\partial T_L}{\partial y}\right)+C_{AO}H_R(1-v_f)\frac{d\alpha}{dt}+\psi_c\left(\frac{I}{A}\right)^2;$$

$$L_b<y\leqslant L_b+L_L\ \text{(laminate)} \tag{4}$$

$$\frac{\partial[(\rho CT)_T]}{\partial t}=\frac{\partial}{\partial y}\left(k_T\frac{\partial T_T}{\partial y}\right);$$

$$L_b+L_L<y\leqslant L_b+L_L+L_T\ \text{(Teflon top plate)}$$

where ρC is the volumetric specific heat, T is the temperature, t and y are the time and location in the mold thickness direction, respectively, k is the thermal conductivity, C_{AO} is the initial concentration of the resin, A is the cross-sectional area in the $x-y$ plane of the resin-saturated carbon mat perpendicular to the direction of the current flow, and v_f is the fiber volume fraction. The subscripts b, L, and T refer to copper base plate, preform layup, and the Teflon top cover, respectively. Additionally, ψ_c is the resistivity of the carbon mat and I is the current passing through it. The thermal conductivity of the resin-saturated carbon mat was obtained by using the mosaic model proposed by Ning and Chou [10], from which the electrical resistivity, ψ, was evaluated by applying Lorenz's law [11] equating thermal and electrical conductivity ratios as follows:

$$\frac{k_c}{k_m}=\frac{\sigma_c}{\sigma_m}=\frac{\psi_m}{\psi_c} \tag{5}$$

where k, σ, and ψ denote the thermal conductivity, the electrical conductivity, and the electrical resistivity, respectively, and the subscripts c and m respectively refer to the resin-saturated carbon mat layer and the matrix resin. It must be mentioned that although Lorenz's law strictly pertains to metals, its applicability to composite materials has been demonstrated in previous studies [12]. Note that the heat generation term due to the resistive heating of the carbon mat is specific to the location where it is being placed, and is zero at all other points in the composite cross section. Further, $d\alpha/dt$ denotes the rate of the cure reaction, which together with the heat of reaction, H_R, determines the heat release rate during the cure process. The expression for the reaction rate is given by the kinetics model, Eq. (1).

The governing equation, Eq. (4), is subject to the following initial conditions in the three regions, namely, the copper plate, the laminate, and the Teflon cover:

$$T_L(y,0)=T_b(y,0)=T_T(y,0)=T_0,\quad \alpha(y,0)=0\ \text{in the laminate,} \tag{6}$$

where T_0 is initial (ambient) temperature. The boundary conditions associated with the governing equations, Eq. (4), are the prescribed cure temperature cycle at the bottom of the copper base ($y=0$ in Fig. 1) and convective heat loss at the top of the Teflon cover ($y=L_b+L_L+L_T$ in Fig. 1). In addition, the temperature and the heat fluxes must be continuous at the composite-copper interface ($y=L_b$) and the composite-Teflon cover interface ($y=L_b+L_L$). These conditions can be represented as follows:

$$T=T_{\text{cure}}(t);\quad y=0$$

$$-kT\frac{\partial T_T}{\partial y}=h(T_T-T_0);\quad y=L_b+L_L+L_T$$

$$T_b=T_L,\quad k_b\frac{\partial T_b}{\partial y}=k_L\frac{\partial T_L}{\partial y};\quad y=L_b \tag{7}$$

$$T_L=T_T,\quad k_L\frac{\partial T_L}{\partial y}=k_T\frac{\partial T_T}{\partial y};\quad y=L_b+L_L$$

where h is the heat transfer coefficient and all other terms in the above equations are as defined previously. The convective heat transfer coefficient on the top plate, h, is obtained by using the correlation for natural convection of quiescent ambient air with constant temperature over a horizontal flat plate configuration [13]. The thermochemical equations, Eqs. (1) and (4), were solved for the temperature and the degree of cure profiles in the composite using an alternating implicit direction (ADI) finite difference method as explained by Rai and Pitchumani [14].

Results and Discussion

The resistive heating experiments were conducted by systematically varying the number of carbon mats, their location in the preform, and the power supplied to them. The objective of the studies was to understand the effects of these variables on the composite fabrication time, the temperature histories during the process, and the microstructural quality of the parts fabricated. It may be recalled that the construction of the experimental apparatus allowed for embedding a maximum of three carbon mats at locations $c1$, $c2$, and $c3$, as shown in Fig. 1. It may be reasoned that since the intent of embedding the resistive elements is to provide supplemental heating to the inner layers of the composite, it is best to position the heating elements at the locations furthest from the base heater. Accordingly, three different placements of the carbon mats were studied. Further, for each of the three placements, two power inputs—9 W and 24 W—representing a low and a high level, respectively, were investigated. The resulting six configurations are listed in Table 1, along with the nomenclature used to identify the different configurations, and the locations of the carbon mats in each case.

The effects of the supplemental heating configurations on the temperature distribution within the composite are shown in Fig. 4 for four of the six configurations, namely, the base case, $1cp1$, $2cp2$, and $3cp1$ (Table 1). A common cure cycle was used for all the cases studied, and was comprised of raising the temperature of the mold base, initially at room temperature, to 130°C within about 300 s and maintaining it at 130°C until the composite was cured. The discrete markers in Fig. 4 represent the temperatures recorded from the experiments at the four thermocouple locations $T1$, $T2$, $T3$, and $T4$ (Fig. 1(*a*)), while the continuous lines represent the model-simulated values for the temperature distributions

Table 1 Heating configurations considered in the studies

Number of carbon mats	Location from the mold base [in.]	Power supplied [W]	Nomenclature
0	–	–	base
1	3/4	9	1cp1
	3/4	24	1cp2
2	3/4, 1/4	9	2cp1
	3/4, 1/4	24	2cp2
3	3/4, 1/4, 1/8	9	3cp1
	3/4, 1/4, 1/8	24	3cp2

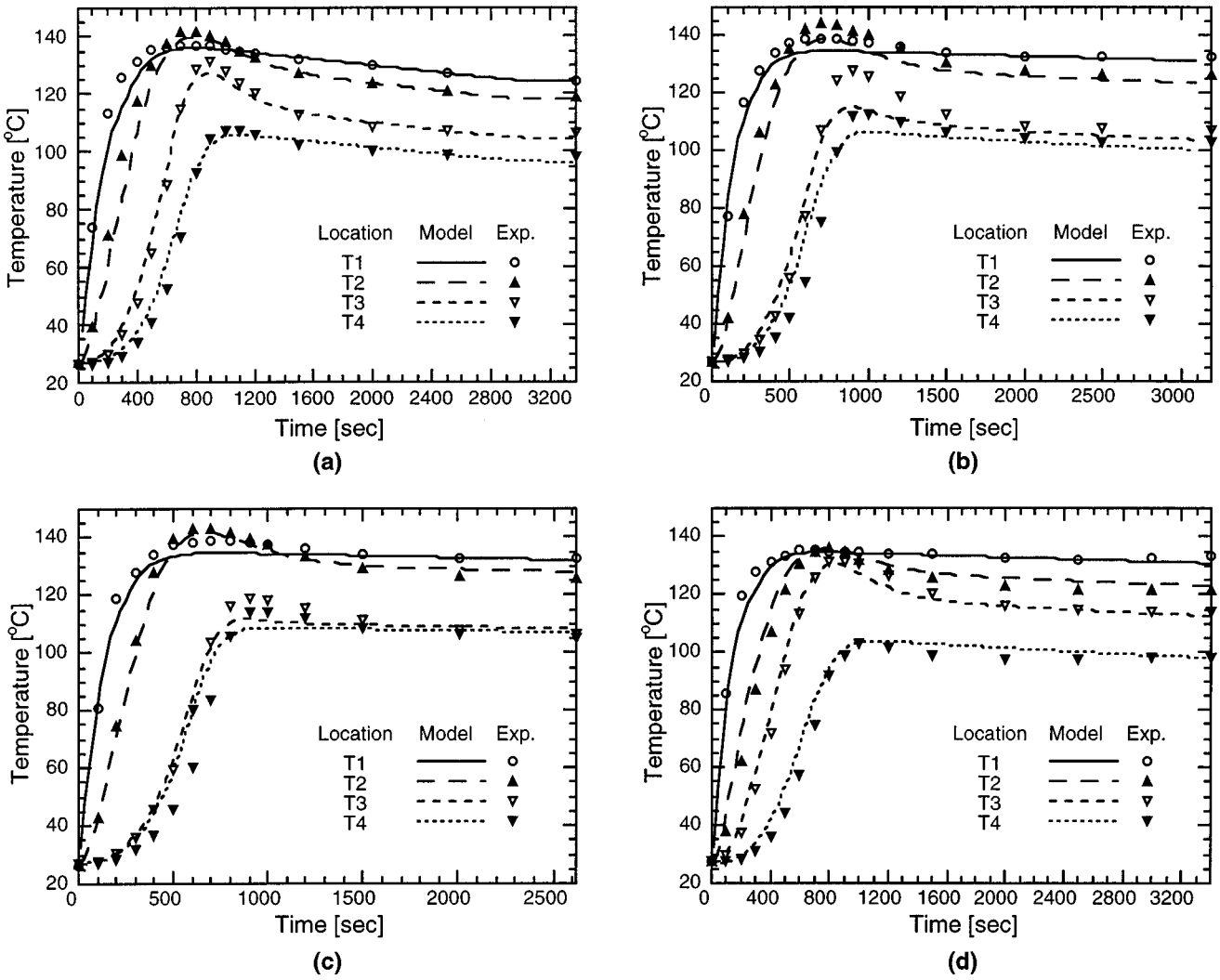

Fig. 4 Variation of the measured and model-predicted temperature histories through the thickness of the composite for (*a*) base heating only, and supplemental heating configurations: (*b*) 1*cp*1, (*c*) 2*cp*2, and (*d*) 3*cp*1

at the same four locations within the composite. As seen in the plots, the model predictions follow the experimental temperature profiles closely for all cases, throughout the cure reaction. The model predicts the magnitude and the location of the exotherm within the composite accurately, to within the experimental error.

As mentioned previously, reducing the cure time is one of the prime objectives of using the supplemental resistive heating elements. However, the resistive heating of the carbon mats may cause locally high temperatures and high temperature gradients. It is also of interest to examine the impact of the supplemental heating on the spatial temperature difference through the thickness of the composite being cured. The high temperatures may degrade the composite, and together with spatial temperature gradients correlate to residual thermal stresses which are detrimental to the product. Furthermore, in some applications, it may be desirable to limit the maximum temporal temperature gradients as a means of controlling the exotherm during the cure reaction. Therefore, in addition to the cure time, the various heating configurations are examined in regard to the maximum temperature, temperature homogeneity through the composite cross section, and the maximum temperature gradient (temporal) in the composite during the process.

The results of the study are summarized in Fig. 5, wherein Fig. 5(*a*) presents the experimentally observed trends, while the data in Fig. 5(*b*) correspond to the numerical simulation of the six different configurations. Further, the results are expressed in Figs. 5(*a*) and 5(*b*) as a percentage change with respect to the base case, in which resistive heating was not included. Positive values on the plots, therefore, denote an increase relative to the base case, while negative values represent a decrease. Overall, the predictions of the process simulations are seen to match well with the experimental trends on each of the parameters which are described below.

Figure 5 shows that the maximum temperature and maximum temperature difference are minimally influenced by the supplemental heating over the range of the power inputs considered. The maximum temperature difference is measured as follows: the difference between the maximum and the minimum temperatures across the cross section is noted at every time during the cure process. The maximum of these temperature difference data constitutes the ΔT_{max} values reported. For most of the configurations studied, the measured values of T_{max} and ΔT_{max} are seen to be within the experimental accuracy. It is evident from the simulation results (Fig. 5(*b*)) that, for a fixed number of carbon mats, the maximum temperature increases, whereas the maximum temperature difference decreases with increasing power input. In particular, the use of a single carbon mat with a power input of 24 W, i.e., the 1*cp*2 configuration, exhibits the largest maximum temperature owing to the highest local power dissipation. Further-

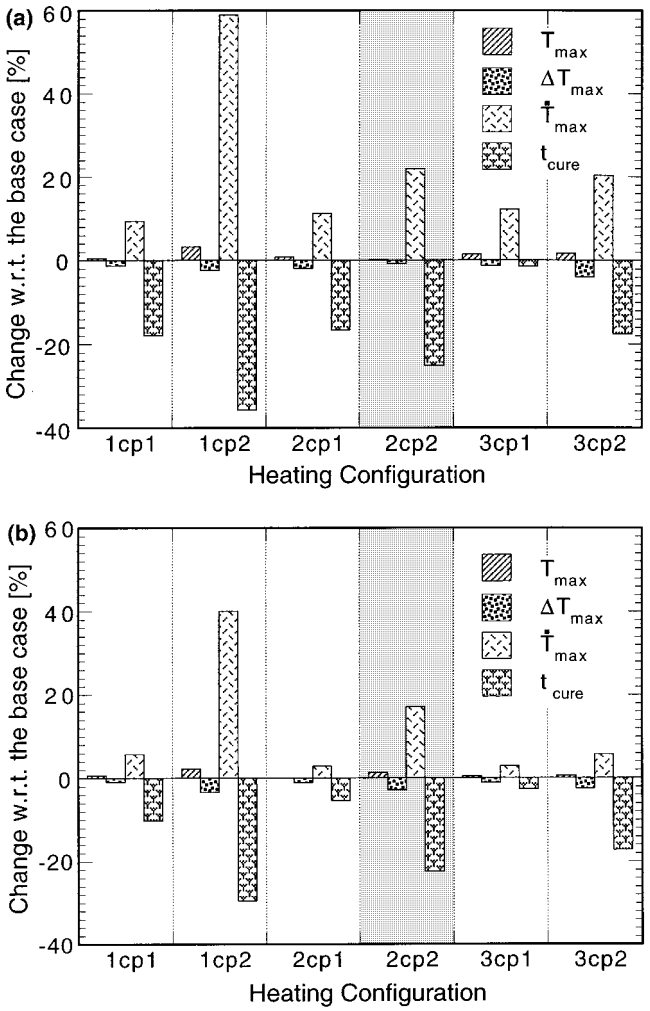

Fig. 5 Comparison of (*a*) experimentally established and (*b*) model-predicted values of the parameters T_{max}, ΔT_{max}, $\dot{T}_{max}$, and t_{cure}, normalized with respect to the base case, for the different heating configurations listed in Table 1

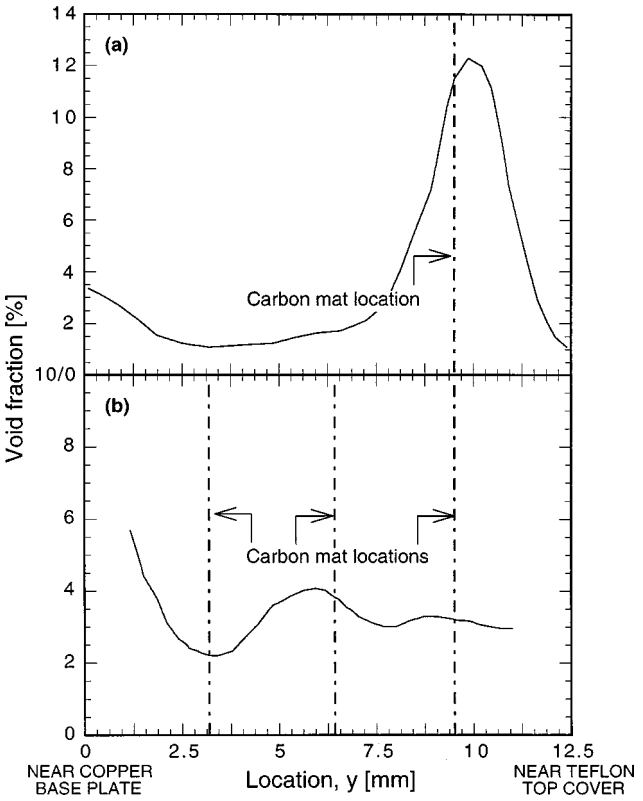

Fig. 6 Variation of the measured void fraction through the thickness of the composite for the supplemental heating configurations: (*a*) $1cp1$ and (*b*) $3cp1$

more, since the $1cp2$ configuration provides the maximum supplemental heating furthest from the base heater, the spatial temperature gradient, ΔT_{max}, is minimized.

Of the six resistive heating configurations studied, the case of a single carbon mat heated with a power of 24 W (i.e., the $1cp2$ case in Table 1) demonstrated the largest value of the maximum temperature gradient. The temperature gradient was found to be principally a function of the rate at which the carbon mat was heated, which is, in turn, a function of the resistance of the carbon mat and the magnitude of the current passing through it. As the number of carbon mats increases, the total current supplied is divided among them, which leads to lower local power dissipation. The case of $1cp2$ corresponds to the supplied power being dissipated entirely in one location, resulting in the highest temperature gradient.

Figure 5 demonstrates that the cure time is reduced with the addition of the resistive heating elements. For a given number of carbon mats, the cure time decreases with increasing power supplied. The cure time savings, however, decrease with increasing number of carbon mats, as seen in Fig. 5. The use of a single carbon mat with a power input of 24 W (the $1cp2$ case), therefore, corresponds to the least cure time, of the cases studied, and represents the optimal arrangement solely from a productivity viewpoint. However, this configuration leads to excessive temperature gradients, which may be undesirable. The $2cp2$ configuration, on the other hand, yields a 25 percent reduction in the cure time with a moderate, more acceptable, increase in the temperature gradient value. The embedding of two carbon mats with a high power supplied to them may therefore be regarded as being optimal based on the processing time and the temperature-related considerations. This configuration is highlighted by the lightly shaded rectangular area in Fig. 5. The trends in the experimental data are corroborated by the simulation results in Fig. 5(*b*).

In addition to the processing considerations, it is important to examine the void content in composites since the voids directly influence the mechanical properties of the composite; a higher void content leads to deterioration of the composite properties. In order to evaluate the void fraction, image analysis was performed through the composite thickness. Seven specimens corresponding to each of the six resistive heating configurations and the base case were sectioned from the composite plaques fabricated. The samples were mounted and polished for microstructural inspection, using standard sample preparation techniques [15]. A suitable magnification was selected so as to clearly resolve the matrix, carbon mat, glass fiber, and the void regions. Using a reflected light source, the representative sections of the microstructure were captured into a 8100/100 AV Power PC Macintosh computer via a Scion image grabber from a Hitachi CCD camera mounted on a Nikon Optiphot microscope. The image analysis software, NIH Image, was used to evaluate the void fractions of the captured digitized images.

Figure 6 presents the void fraction distribution across the thickness of the composite specimens for two representative cases: the $1cp1$ and the $3cp1$ heating configurations. The chain-dashed lines in the plots denote the locations of the carbon mats. Overall, it is observed that the void fraction is higher in the vicinity of the carbon mats. This may be attributed to the localized heating and the resulting vaporization of the volatile contents in the epoxy matrix around the resistive elements. The maximum void fraction

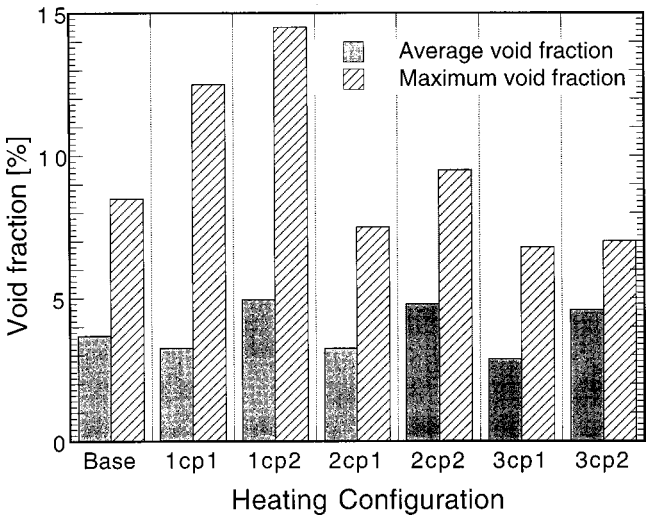

Fig. 7 Variation of the average and maximum void fractions in the composite specimens for the seven configurations listed in Table 1

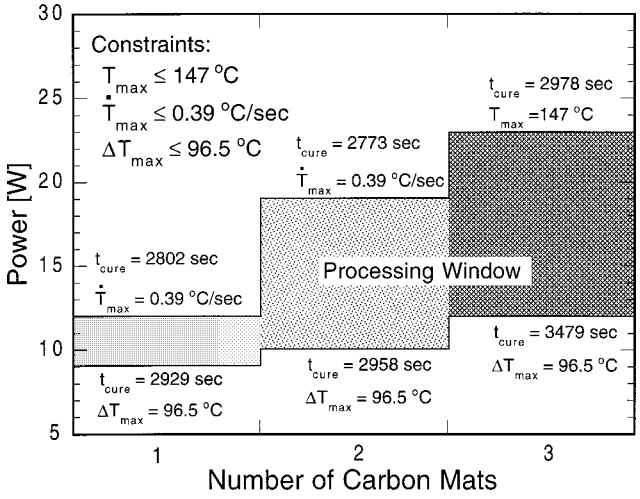

Fig. 8 Processing window on the feasible range of power inputs, obtained from the experimental study

is seen to be high for the case of resistive heating using single carbon mat (Fig. 6(*a*)) since the input power is dissipated entirely in one location. The distribution of the power supplied among three resistive elements, on the other hand, leads to lower void fraction values (Fig. 6(*b*)).

Figure 7 summarizes the maximum void fraction and the average void fraction through the specimen thickness, for each of the seven cases in Table 1. As observed, the void fraction increases by about 2 percent with increasing power supplied. The average void fraction ranges from 3 percent (for the lower power cases) to 5 percent (for the higher power cases). The maximum void fraction is the highest for the cases involving a single carbon mat, wherein resistive heating is intensely localized and consequently leads to high temperatures. For all the other cases, the maximum void fraction is seen to be less than 10 percent %. Figure 7 further reveals the trend that for a given power (either 9 or 24 W) the average and the maximum void fractions decrease with increasing number of carbon mats, owing to the distribution of the resistive heating through the thickness.

It is evident from Fig. 7 that the $2cp2$ configuration, which was seen to be optimal based on the results in Fig. 5, corresponds to a maximum void fraction of about 9.5 percent and an average void content of 5 percent. An alternative configuration of embedding two carbon mats with a low power input, the $2cp1$ case, yields a marginal reduction of about 2 percent on the void fractions; however, the cure time savings are significantly diminished, as seen in Fig. 5(*b*). It may, therefore, be qualitatively reasoned that the use of two carbon mats with a high power input (i.e., $2cp2$) represents the best supplemental heating scenario over the range of power inputs studied.

The measured temperature data from the experiments was also used to obtain processing windows that represent the feasible range of power inputs as a function of the number of embedded carbon mats, for maintaining the maximum values of the temperature, the temperature difference, and the temperature gradient within specified limits (*constraints*). The construction of the processing windows is as follows: For a fixed number of carbon mats, a linear variation was assumed for each of the parameters—$T_{\max}$, $\Delta T_{\max}$, $\dot{T}_{\max}$, and t_{cure}—between the two power inputs studied (9 and 24 W). For specified values of the constraints, upper and lower bounds on the power were then determined by superimposing the inequality constraint specifications on the assumed linear variations. This yielded three permissible ranges of power for resistive heating using one, two, and three carbon mats.

Figure 8 shows the processing window obtained based on the experiments conducted. The abscissa represents the number of carbon mats used while the ordinate shows the feasible range of power. The values of the constraints on $T_{\max}$, $\Delta T_{\max}$, and $\dot{T}_{\max}$ used to obtain the processing windows are given in the figure. The shaded bands in the plot indicate the range of acceptable power inputs which satisfies the specified constraint values. Toward maintaining the temperature difference within the permissible limit, a minimum amount of power is required to be supplied to the laminate. Accordingly, the lower bounds are seen to be governed by the allowable temperature difference within the composite (which was taken to be 96.5°C in this study). The upper bounds, however, are determined by the constraints on the maximum allowable temperature gradient (0.39°C/s) and the maximum temperature within the composite during cure (147°C). As noted earlier, increasing the number of resistive carbon mats embedded within the composite leads to a reduced local power dissipation within each mat. This implies that a larger power may be used without violating the constraints. The maximum and the minimum permissible power are therefore seen to increase with increasing number of carbon mats, although the shift is less pronounced for the lower bound.

The cure time values associated with the upper and lower bounds are also indicated in Fig. 8. It is clear that the upper bound corresponds to the maximum permissible power and, therefore, to the least cure time for a fixed number of carbon mats. From a comparison of the cure time values, it follows that the use of two carbon layers, at its upper bound on the power (about 19 W), is the optimum configuration which minimizes the cure time as well as satisfies the imposed constraints. The corresponding void fractions may be obtained from a linear interpolation of the data in Fig. 7 between the two power levels of 9 and 24 W to be 8.8 percent (maximum) and 4.3 percent (average). It is noteworthy that the two-carbon heating configuration derived as being optimum from the processing windows is in agreement with the optimum inferred qualitatively earlier from Figs. 5–7.

Additional constraints, such as process capability, may be added toward obtaining a more refined process window. Furthermore, process simulations conducted over a wide range of parameters may be used to obtain a better estimate of the processing window and the optimum parameters, as presented in a companion study by Zhu and Pitchumani [16,17]. These studies also reveal a greater sensitivity of parameters, such as the maximum temperature difference to the heating configurations, over a range of power densities outside those discussed in this paper. The interested reader is referred to Zhu and Pitchumani [16,17] for fur-

ther details. The present study investigated the use of a constant current through the cure process. Due to the exothermic nature of the cure process, the supplemental resistive heating could potentially be tapered off after initiation of sufficient exotherm. The suggests that an optimum current cycle along with an optimum cure temperature cycle may be obtained for maximizing process efficiency. Such strategies are presently being explored and will be reported in the future.

Conclusions

The use of embedded carbon mats as internal resistive heating elements was explored as a means of accelerating the cure process. Experiments as well as numerical process simulations were conducted for a range of combinations of power inputs and carbon mat placements within the composite. A processing window was presented toward identifying the range of acceptable power that can be supplied for a given placement of the carbon mats, without violating specified constraints influencing product quality. The studies revealed that use of a single carbon mat with a high power input leads to the shortest cure time, but also corresponds to excessive internal temperature gradients during the process, and a large void content in the composite product. Based on the configurations and the parameter ranges studied, embedding two internal heating elements with a high power input was determined to be optimal from the viewpoint of reducing cure time while maintaining the maximum temperature gradient, maximum temperature, temperature homogeneity, and maximum void fraction within acceptable limits.

Acknowledgments

The authors gratefully acknowledge the financial support for the project provided by the National Science Foundation through Grant No. DMI-9522801 and the Office Naval Research through a Young Investigator Award (Contract No. N00014-96-1-0726) with James J. Kelly as the Program Officer. The Owens/Corning Fiberglass corporation and the Shell Chemical Company are acknowledged for donating the materials used in the study.

Nomenclature

A = cross-sectional area of the carbon mat perpendicular to direction of the current flow ($in.^2$)
C = specific heat (kJ/kg K)
E_1, E_2 = activation energies in the kinetics model ($kJ\,mol^{-1}$)
h = heat transfer coefficient ($W/m^2\,K$)
H_R = heat of the cure reaction (kJ/kg)
I = current passing through the carbon mat (amp)
k = thermal conductivity (W/mK)
k_{10}, k_{20} = frequency factors in the kinetics model (s^{-1})
T = temperature in the composite (K)
t = time (s)
v_f = fiber volume fraction
x, y, z = coordinate axes

Greek Symbols

α = degree of cure
ψ = resistivity of the carbon mat (m)
ρ = density (kg/m^3)
m, n = empirical exponents in the cure kinetics model (Eq. (1))

Subscripts

b = copper
L = laminate
T = Teflon

References

[1] Carrozino, S., Levita, G., Rolla, P., and Tombari, E., 1990, ''Calorimetric and Microwave Dielectric Monitoring of Epoxy Resin Cure,'' Polym. Eng. Sci., **30**, pp. 366–373.
[2] Lee, W. I., and Springer, G. S., 1984, ''Interaction of Electromagnetic Radiation with Organic Matrix Composites,'' J. Compos. Mater., **18**, pp. 357–386.
[3] Lee, W. I., and Springer, G. S., 1984, ''Microwave Curing of Composites,'' J. Compos. Mater., **18**, pp. 387–409.
[4] Butler, D., and Engel, R. S., 1994, ''On the use of Embedded Graphite Patches for Cure in Resin Transfer Molding,'' in *Proceedings, ICCM-10*, Whistler, Canada, pp. 269–275.
[5] Sancaktar, E., Weijian, E. M., and Yurgartis, S. W., 1993, ''Electric Resistive Heat Curing of the Fiber-Matrix Interface in Graphite/Epoxy Composites,'' ASME J. Mech. Des., **115**, pp. 53–60.
[6] VanDerSchuur, L., and Pitchumani, R., 1997, ''A LabVIEW-based Process Control System for Composites Fabrication,'' presented at the LabVIEW Virtual Instrumentation Education Conference, MIT, Cambridge, MA, May.
[7] Han, C. D., Lee, D. S., and Chin, H. B., 1986, ''Development of a Mathematical Model for the Pultrusion Process,'' Polym. Eng. Sci., **26**, pp. 393–404.
[8] Lem, K. W., and Han, C. D., 1983, ''Chemorheology of Thermosetting Resin,'' J. Appl. Polym. Sci., **28**, pp. 3155–3183.
[9] Kamal, M. R., and Sourour, S., 1976, ''DSC of Epoxy Cure: Isothermal Kinetics,'' Thermochim. Acta, **14**, pp. 41–59.
[10] Ning, Q., and Chou, T.-W., 1995, ''A Closed-Form Solution of the Transverse Effective Thermal Conductivity of Woven Fabric Composites,'' J. Compos. Mater., **29**, pp. 2280–2294.
[11] Condon, E. U., and Odishaw, H., 1967, *Handbook of Physics*, McGraw-Hill, New York.
[12] Pitchumani, R., Liaw, P. K., Yao, S. C., Jeong, H., and Hsu, D. K., 1995, ''Theoretical Models for the Anisotropic Conductivities of Two-Phase and Three-Phase Metal-Matrix Composites,'' Acta Metall. Mater., **43**, pp. 3045–3059.
[13] Incopera, F. P., and DeWitt, D. P., 1996, *Fundamentals of Heat and Mass Transfer*, Wiley, New York.
[14] Rai, N., and Pitchumani, R., 1997, ''Optimal Cure Cycles for the Fabrication of Thermosetting-matrix Composites,'' Polym. Compos., **18**, pp. 556–581.
[15] Russ, J. C., 1995, *The Image Processing Handbook*, CRC, Boca Raton, FL.
[16] Zhu, L., and Pitchumani, R., 1999, ''Processing Envelopes for Supplemental Internal Resistive Heating during Thermosetting-Matrix Composite Cure,'' J. Reinf. Plast. Compos., **18**, No. 13, pp. 1242–1253.
[17] Zhu, L., and Pitchumani, R., 1999, ''Analysis and Design of a Thermosetting Matrix Cure Process with Supplemental Internal Resistive Heating,'' Compos. Sci. Technol., submitted.